Geoderma 340 (2019) 81–93

Contents lists available at ScienceDirect

Geoderma

journal homepage: www.elsevier.com/locate/geoderma

Andosolization of ferrallitic soils in the Bambouto Mountains, West Cameroon

E. Van Ranst[a,*], M. Doube[b], F. Mees[c], M. Dumon[a], L. Ye[a], B. Delvaux[d]

[a] Ghent University, Department of Geology (WE13), Gent, Belgium
[b] University of Dschang, Department of Soil Science, Dschang, Cameroon
[c] Royal Museum for Central Africa, Department of Geology and Mineralogy, Tervuren, Belgium
[d] Université catholique de Louvain, Earth and Life Institute – Soil Science, Louvain-la-Neuve, Belgium

ARTICLE INFO

Handling editor: Michael Vepraskas

Keywords:
Andic properties
Soil organic matter
Ferrallitic soils
Umbrisols

ABSTRACT

Soils along a toposequence (1500–2260 m) on the southern slope of the volcanic Bambouto Mountains in western Cameroon were investigated to elucidate the occurrence and development of andic properties at high altitude (> 1800 m) in the study area. The surface layer that has these properties has in the past been interpreted as a weathered volcanic ash layer, overlying ferrallitic soils that developed from lava flow deposits and derived pediments. Physico-chemical and mineralogical data demonstrate that the andic properties of the high-altitude pedons result from SOM accumulation, favoured by climate and vegetation. The 'andosolization' process affecting these profiles involves the formation of organo-metallic complexes, which is mediated by organic ligands and controlled by the dissolution of gibbsite and iron oxides. Increasing andosolization with increasing altitude, due to SOM accumulation, is well reflected by soil classification names, especially by the humic qualifier for the soils below 1800 m a.s.l. and the protoandic subqualifier for the soils at higher altitude. All analysed properties show features that are incompatible with derivation of the upper part of the high-altitude pedons from volcanic ash. In studies of soils from similar settings, care should be taken to avoid misinterpretation of surface horizons marked by environmentally conditioned development of organo-metallic complexes as ash-derived layers.

1. Introduction

In Cameroon, volcanic ash soils classified as Andosols occupy a rather small area along the Cameroon Volcanic Line (CVL), surrounded by areas with predominantly ferrallitic soils (Sieffermann, 1973; Delvaux et al., 1989). Ferrallitic soils are also the major soils of the West Cameroon highlands, characterized by a wet, humid tropical climate (Van Ranst et al., 1998). Among these highlands, the Bambouto Mountains are the third most important volcanic complex of the CVL in volume, after Mounts Cameroon and Manengouba. Soil surveys along the southern slope of the Bambouto Mountains have reported ferrallitic soils that are mainly derived from basaltic and trachytic parent materials, but showing andic soil properties above 1800 m altitude (Doube and Van Ranst, 1984; Van Ranst et al., 1987; Tematio et al., 2004; Tematio, 2005). Doube and Van Ranst (1984) assumed that the soils above 1800 m developed on volcanic ash covering ferrallitic soils that formed on pediments. The assumed volcanic ash soils were classified as Oxic Dystrandepts (Doube, 1989), following the then-current version of Soil Taxonomy (Soil Survey Staff, 1987). Tematio et al. (2004) subdivided the soils along the southern slope of the Bambouto Mountains into three major soil groups with decreasing altitude: andic soils, andic ferrallitic soils and ferrallitic soils. The first group, classified as Andosols, dominates at high altitudes (> 2000 m), and the second group, combining both ferrallitic and andic soil properties, is dominant at somewhat lower altitude (1600–2000 m). More recent studies classify the soils above 2000 m as Andosols or Andisols (Tematio et al., 2011; Temgoua et al., 2014), but these studies do not present the data required to verify their classification according to Soil Taxonomy or WRB, or to understand their genesis.

Dumort (1968) and Morin (1989) proposed that late Pleistocene volcanic ashes (ca. 15,000 BP), probably derived from explosive eruptions at the eastern edge of the Bamiléké plateau, cover the volcanic cone of the Bambouto Mountains. However, no data support this hypothesis. Besides, volcanic ash deposits are not expected in a basaltic-trachytic volcanic system. The influence of volcanic ash on local soils thus remains open to debate. Consequently, development of andic properties through genetic processes other than volcanic ash weathering cannot be excluded. Andic soil properties can indeed develop in

* Corresponding author at: Department of Geology (WE13), Ghent University, Krijgslaan 281 (S8), B-9000 Gent, Belgium.
E-mail address: eric.vanranst@ugent.be (E. Van Ranst).

https://doi.org/10.1016/j.geoderma.2018.12.024
Received 28 August 2018; Received in revised form 12 December 2018; Accepted 13 December 2018

the upper part of strongly weathered lateritic formations (Subramanian and Mani, 1981; Caner et al., 2000, 2003, 2007, 2011). When environmental conditions, particularly climate and vegetation, promote SOM accumulation in highly weathered soils, gibbsite and iron oxides are potential sources of Al and Fe to form organo-metallic complexes. This process can generate andic soil properties, leading to the formation of non-allophanic, non-volcanic Andosols on top of highly weathered soils with high gibbsite content (Subramanian and Mani, 1981; Caner et al., 2000).

The main objective of this study is to elucidate the origin and formation of andic properties in soils along the upper southern slope of the Bambouto Mountains, considering two possible pathways: (i) weathering of a volcanic ash deposit, and (ii) iron and aluminium release associated with SOM accumulation, with formation of stable organo-metallic complexes. We hypothesize that a detailed study of micromorphological, physico-chemical and mineralogical characteristics of soils at various altitudes along the mountain slope can allow us to understand the andosolization process in this volcanic region.

2. Setting

2.1. Geological context

The Bambouto Mountains, West Cameroon (9°57′ to 10°15′E, 5°27′ to 5°48′N) constitute an elongated shield complex with a diameter of 25 km (E-W) to 50 km (SW-NE). The base of the massif is at about 1500 m a.s.l., where it overlies a metamorphic Precambrian basement complex of gneiss, migmatites and anatexites (Tchoua, 1974). The massif culminates in a large caldera at 2680 m. The Bambouto volcanic cone (Mount Mélétan, 2740 m) originated during the Upper Miocene (Morin, 1989). The complex consists of various volcanic deposits, dated between 21.12 Ma and 0.5 Ma (Woolley, 2001; Gountié Dedzo et al., 2011), comprising basalt, trachyte, phonolite, and rhyolite, in the form of tuff, breccia, and ignimbritic deposits, representing various facies (Tchoua, 1968, 1973; Youmen, 1994; N'ni and Nyobe, 1995; Marzoli et al., 1999, 2000; Nono et al., 2003, 2004). The ignimbrites of the Bambouto region were derived from a caldera-forming eruption (15.5 Ma) that generated pyroclastic flows, close to pyroclastic surges. Lithic fragments were incorporated along the base of the pyroclastic flow, with associated co-ignimbrite ash deposits produced by winnowing (Nono et al., 2004). Dumort (1968) and Morin (1989) assume that the volcanic cone is covered by Late Pleistocene volcanic ash deposits (ca. 15,000 BP; up to 1 m), probably derived from explosive eruptions at the eastern edge of the Bamiléké plateau.

2.2. Environmental setting

The study area is located south of the Bambouto caldera, where a toposequence was sampled along the southern slope of the volcanic cone (15 km length, 2410–1500 m altitude) (Fig. 1). The landscape comprises two main units: (i) the Bamiléké plateau (1400–1640 m a.s.l.), where an Oligocene volcanic sheet (trachytic tuff and basalt) overlies the Precambrian basement complex (Hieronymus, 1972; Regnoult, 1986), and (ii) the Miocene Bambouto volcanic cone (trachyte and basaltic flows). During the Pliocene and Pleistocene, the Bamiléké plateau was exposed to weathering and erosion for long periods of time, resulting in the development of extensive lateritic plains, dissected by rivers. Those plains developed mainly on basalt, but also on basement complex rocks and tuff deposits. Only remnants of those plains are now present, generally as isolated hills. The Bambouto volcanic cone is characterized by numerous escarpments exposing trachytic rocks, with associated weakly sloping piedmont plains on highly weathered bedrock. The altitude ranges from 1700 to 2740 m above sea level (Van Ranst et al., 1998).

Mean annual precipitation (MAP) along the southern flank of the Bambouto volcano is 1918 ± 255 mm (Kengni et al., 2009). MAP is highest at the Mount Mélétan cone (2507 mm), and it sharply decreases with decreasing altitude from north to south. Two distinct seasons occur, with negligible rainfall from December to February. The climate of the zone above 2000 m is pseudo-tropical, with temperate characteristics due to altitude (Morin, 1988). Mean monthly temperatures vary from 10 to 12 °C. The climate in this zone is cool and humid, characterized by frequent mist and fog.

Open grassland savanna (Morin, 1988), in the form of *Sporobolus* prairies common in temperate environments (Tsozué et al., 2009), was the original vegetation. Human activity has strongly impacted this vegetation through raffia cutting and wood harvesting, farming, and cattle rearing, resulting in an open vegetation with scattered shrubs. Intensive agriculture is predominant, with maize, beans, potatoes and tea as main crops (Morin, 1988; Kuété, 1999). Scarce fallow lands are dominated by *Pteridium aquilinum*, *Rafia vinifera*, *Eucalyptus grandis*, *Imperata cylindrica*, and *Pennisetum purpureum*. Intensification of agriculture in the Bambouto highlands is driven by increasing human population (Bitondo et al., 2013); the soils are increasingly used for growing Irish potatoes and carrots (which constitute > 70% of the produce), while cattle rearing is disappearing.

3. Materials and methods

3.1. Soil sampling

Several transects were carried out along the southern slopes of the Bambouto massif, with full description of soil augerings, to select representative pedons along a toposequence (1500–2260 m altitude) (Fig. 2). The selected pedons were described according to FAO guidelines (FAO-ISRIC, 1990), using the Munsell Color Chart to define soil colour. Bulk samples and oriented undisturbed samples were collected for each soil horizon.

3.2. Physico-chemical analyses

Bulk samples were air-dried and crushed to pass through a 2-mm sieve. Physical and chemical analyses were performed for the air-dried fine earth fraction (< 2 mm), according to the procedures outlined by van Reeuwijk (2002) unless otherwise specified. Particle size distribution was determined by the pipette method after removal of organic matter (H_2O_2) and disaggregation of pseudosilt (0.01 N HCl). Organic carbon (OC) content was determined by the Walkley and Black method. Soil pH was measured in soil:H_2O and soil:KCl (1 M) suspensions, using a soil:liquid ratio of 1 g:2.5 mL. Cation exchange capacity (CEC) and exchangeable base cations were determined by leaching with 1 M ammonium acetate (NH_4OAc, pH 7), using a Centurion mechanical vacuum extractor. The concentrations of exchangeable base cations in the leachate were measured with ICP-OES. Exchangeable acidity (Al + H) was determined by titration of a 1 M KCl percolate, whereas exchangeable Al was measured in the percolate with ICP-OES. Extractable acidity was determined by titration following treatment with a $BaCl_2$-TEA (tri-ethanolamine) buffer solution at pH 8.2. Base saturation (BS) was calculated from the sum of contents of exchangeable base cations (SBC), relative to CEC determined with 1 N NH_4OAc at pH 7 (BS-NH_4OAc) and relative to CEC determined by sum of cations (SBC + extractable acidity) (BS-SC).

Bulk density (BD) was determined on oven-dry weight basis for core samples. The phosphate retention percentage in acid media was determined by the method of Blakemore et al. (1981). Selective extractions of Fe, Al, and Si were carried out using ammonium oxalate (o), dithionite-citrate-bicarbonate (d) and sodium pyrophosphate (p) extraction methods (Dahlgren, 1994); Fe, Al and Si concentrations of the extracts were measured by ICP-OES.

The total elemental composition of the fine earth fraction (< 2 mm) was determined after fusion with lithium metaborate at 950 °C, followed by dissolution in 4% HNO_3. Concentrations were measured using

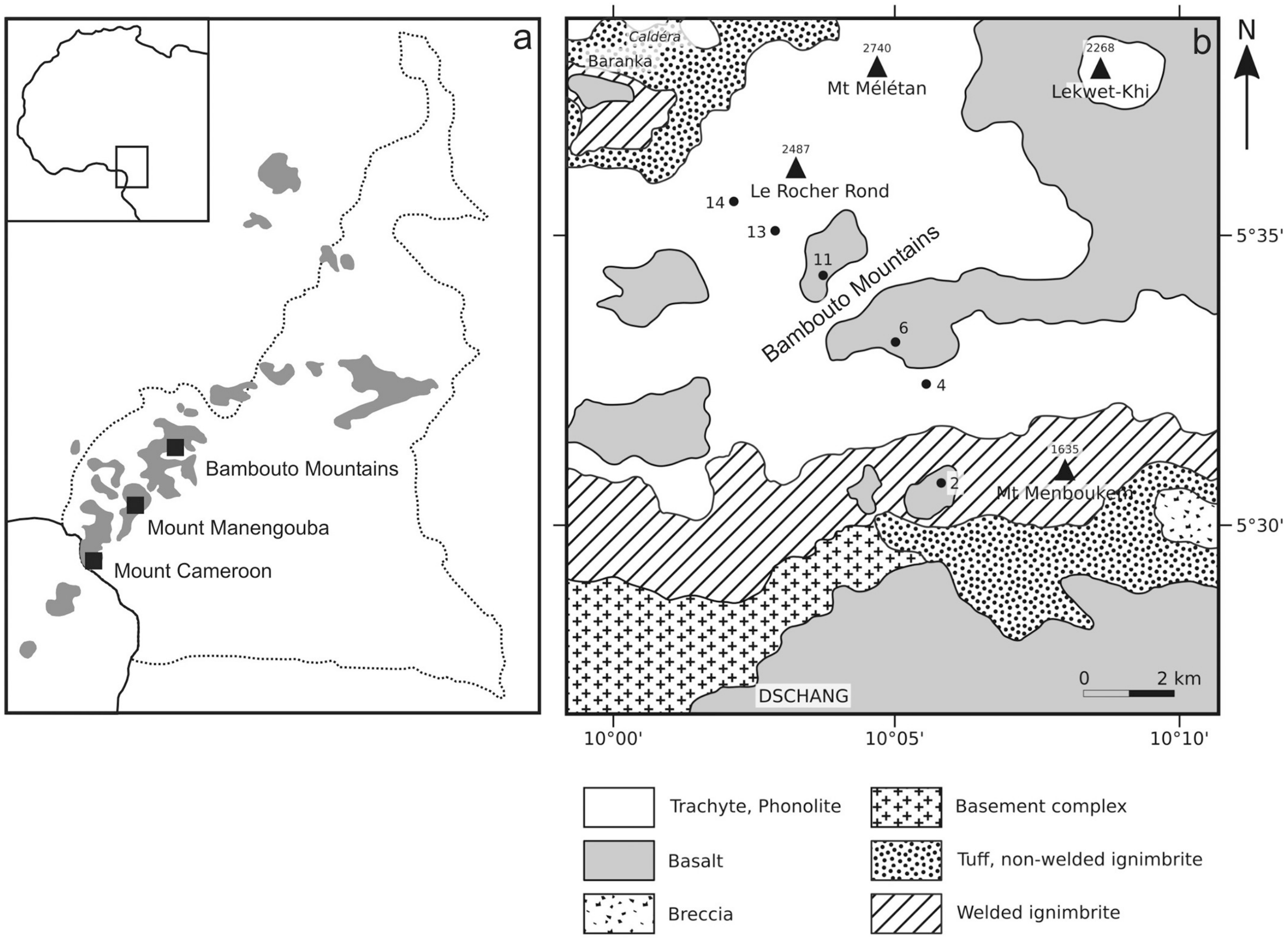

Fig. 1. Profile location. (a) Location of Cameroon Volcanic Line deposits (gray), including the Bambouto Mountains, within Cameroon; (b) Geological sketch map of the southern slope of the Bambouto Mountains, with location of six representative pedons selected for this study.

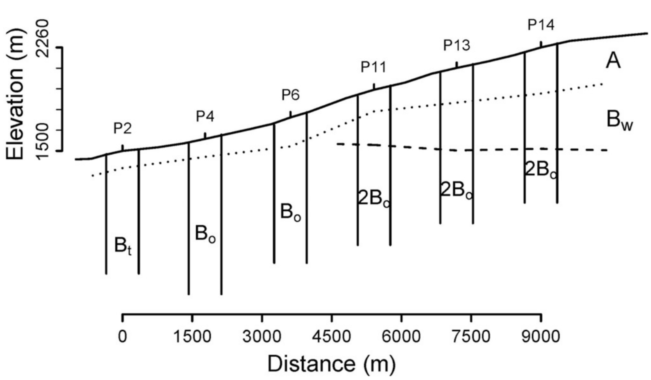

Fig. 2. Location and horizonation of the selected pedons along the toposequence.

ICP-OES. Loss on ignition (LOI) analyses were performed by heating the samples at 105 °C and at 1000 °C. These results were used to aid in quantitative XRD analysis (see further). The contents of alkaline and alkaline-earth cations were summed to compute the total reserve in bases (TRB), which estimates the content of weatherable minerals (Herbillon, 1986).

3.3. Mineralogical analyses

The sand fraction was separated by wet sieving (50 μm) after OM removal (6% NaOCl, pH 8; Siregar et al., 2005) and studied using a polarizing microscope. The silt and clay fractions were separated by successive sedimentation with 2% Na_2CO_3 as dispersant, followed by removal of salts by dialysis.

XRD analysis was performed for bulk, silt and clay samples. Prior to micronizing using a McCrone mill, NaOCl-treated bulk samples (< 2 mm) were gently crushed using a mortar and pestle to pass a 50 μm sieve. Before milling, samples were spiked using 5 wt% ZnO. Ethanol was added as grinding fluid. After milling for 5 min, the obtained slurry was poured into an airbrush jar and spray-dried at 10 to 12 psi (0.7 to 0.8 bar) in a custom-built oven operated at 60 °C (Hillier, 1999). The spray-dried powder was recovered at the bottom of the oven on glossy paper. This powder was then transferred to a sample holder, avoiding to exert pressure during sample loading. For the clay fraction, oriented samples were also used. Some clay and silt samples were reanalysed after heating at 350 °C for 2 h, and some clay samples were reanalysed after formamide treatment (Churchman et al., 1984).

XRD patterns were collected with a Bruker D8 ECO Advance system, equipped with a Cu tube anode and an energy-dispersive position-sensitive LynxEye XE detector. The incident beam was automatically collimated to an irradiated length of 17 mm for powder samples and 15 mm for dried suspensions. The tube was operated at 40 kV and 25 mA. The patterns were collected in a θ–2θ geometry from 3° 2θ to

Table 1
Morphological and physico-chemical properties of the soil horizons of the selected pedons.

Pedon	Hor.	Depth (cm)	Colour		Clay 0–2 (%)	Silt 2–50 (%)	Sand 50–2000 (%)	Class USDA	OC (%)	pH (1:2.5)		ΔpH*	NH$_4$OAc pH 7						BS (%)		Exch. Acid.	Extr. Acid. BaCl$_2$-TEA
													CEC	Ca	Mg	K	Na	SBC				
			Moist	Dry						H$_2$O	KCl		cmol(+)kg^{-1}						NH$_4$OAc	SC	cmol(+)kg^{-1}	
P2 (1500 m)	Ap1	0–6	5YR3/3	5YR4/4	33	57	10	SCL	3.1	5.8	5.2	−0.6	24.4	6.4	2.9	3.00	0.01	12.31	50	67	0.44	6.2
	Ap2	6–18/24	5YR3/3	5YR4/6	51	43	6	SC	3.3	5.5	5.1	−0.4	13.6	6.6	2.6	0.80	0.01	10.01	74	63	0.17	6.0
	Bt1	18/24–32/34	5YR3/4	5YR4/6	58	36	6	C	2.4	5.4	4.9	−0.5	13.6	5.8	2.3	0.40	0.01	8.51	63	58	0.11	6.2
	Bt2	32/34–67	2.5YR3/6	2.5YR4/8	70	27	3	C	1.3	5.3	5.3	0.0	6.9	2.4	1.1	0.30	0.01	3.81	55	76	0.12	1.2
	Bt3	67–103	2.5YR3/6	2.5YR4/8	70	27	3	C	1.0	5.4	5.8	0.3	4.6	1.6	0.9	0.10	0.01	2.61	57	65	0.08	1.4
	Bt4	103–150	10R3/4	2.5YR4/8	76	20	4	C	0.8	5.6	5.9	0.3	7.9	1.6	1.1	0.05	0.01	2.76	35	46	0.04	3.3
P4 (1700 m)	Ap	0–22	5YR2.5/2	7.5YR4/4	38	55	7	SCL	4.3	5.5	4.8	−0.7	24.5	7.8	2.6	0.46	0.01	10.87	44	35	0.28	19.8
	AB	22–40/47	10R3/4	5YR3/4	52	45	3	SC	3.8	5.3	4.8	−0.5	16.3	5.0	2.0	0.24	0.01	7.25	45	33	0.17	15.0
	Bo1	40/47–70	2,5YR3/6	2.5YR4/8	63	35	2	C	2.7	5.3	5.1	−0.2	6.9	2.3	1.2	0.37	0.01	3.88	56	24	0.05	12.2
	Bo2	70–108	2.5YR3/6	2.5YR4/8	65	33	2	C	2.3	5.6	5.5	−0.1	6.8	1.8	0.9	0.32	0.01	3.03	46	20	0.03	12.1
	Bo3	108–136	2.5YR3/6	2.5YR4/8	59	39	2	C	2.2	5.5	5.6	0.1	5.8	1.6	1.0	0.17	0.01	2.78	48	44	0.04	3.6
	Bo4	136–190	10R3/6	2.5YR4/8	62	37	1	C	2.1	5.3	5.5	0.2	5.7	1.5	0.9	0.34	0.01	2.75	47	35	0.05	5.0
P6 (1780 m)	Ap	0–12/18	5YR3/4	7.5YR4/4	76	19	5	C	4.4	5.1	4.4	−0.7	19.6	4.2	2.1	0.40	0.06	6.76	34	23	0.67	22.9
	BA	12/18–32/39	5YR3/6	5YR4/6	83	12	5	C	3.7	5.1	4.7	−0.4	10	2.7	1.4	0.20	0.06	4.36	43	30	0.24	10.4
	Bt1	32/39–52/67	2.5YR3/6	2.5YR4/8	85	11	4	C	2.6	4.9	5.0	0.1	8.8	2.5	1.1	0.05	0.05	3.70	42	41	0.08	5.3
	Btcs2	52/67–88/100	2.5YR3/6	2.5YR4/8	83	11	6	C	2.2	5.1	5.0	−0.1	5.6	1.7	1.0	0.08	0.07	2.85	50	29	0.01	6.9
	2Bo1	88/100–110/128	2.5YR3/6	2.5YR4/8	83	11	6	C	2.0	5.1	5.5	0.4	6.4	1.8	1.2	0.07	0.06	3.13	48	40	0.03	4.6
	2Bo2	110/128–178	2.5YR3/6	2.5YR4/8	81	13	6	C	1.9	5.1	5.5	0.4	8.9	1.6	1.1	0.06	0.06	2.82	31	30	0.02	6.5
P11 (2000 m)	A	0–25/28	5YR2.5/2	7.5YR3/4	66	28	6	C	6.3	5.4	4.6	−0.8	45.4	8.4	2.4	0.40	0.10	11.30	25	29	0.51	28.3
	Bw1	25/28–44/52	7.5YR2.5/2	7.5YR3/4	65	30	5	C	5.3	5.5	4.9	−0.6	42.4	10.7	2.8	0.20	0.10	13.80	33	41	0.14	20.1
	Bw2	44/52–63/72	7.5YR2.5/2	7.5YR3/4	75	21	4	C	4.4	5.6	5.0	−0.6	38	10.4	2.3	0.30	0.01	13.01	34	45	0.14	16.1
	Bw3	63/72–77/84	2.5YR3/8	7.5YR3/4	88	9	3	C	4.1	5.6	5.0	−0.6	33.9	12.4	2.4	0.30	0.01	15.11	45	42	0.20	20.8
	2Bo	77/84–190	2.5YR3/8	5YR4/6	73	25	2	C	4.2	5.5	5.0	−0.5	24.7	8.2	1.6	0.40	0.01	10.21	41	40	0.11	15.0
P13 (2120 m)	A1	0–15/25	5YR2.5/1	7.5YR3/3	85	12	3	C	11.4	5.1	4.4	−0.7	45.3	4.7	2.4	1.10	0.06	8.26	18	17	0.98	41.4
	A2	15/25–42/43	10YR2/2	7.5YR3/3	74	21	5	C	7.1	5.3	4.7	−0.6	38.8	4.6	1.4	0.30	0.06	6.36	17	12	0.32	44.7
	Bw1	42/43–52/54	5YR3/3	7.5YR3/4	87	11	2	C	4.2	5.0	4.6	−0.4	24.4	1.9	1.3	0.30	0.06	3.56	15	12	0.27	26.4
	Bw2	52/54–101	5YR3/4	7.5YR3/4	78	20	2	C	3.6	5.0	4.9	−0.1	14.4	1.0	0.7	0.07	0.06	1.83	13	13	0.06	12.3
	2Bo1	101–131	2.5YR3/6	2.5YR4/8	81	17	2	C	2.2	4.9	5.0	0.1	6.2	1.3	0.4	0.03	0.05	1.78	29	46	0.06	2.1
	2Bo2	131–190	2.5YR3/6	2.5YR4/8	80	17	3	C	1.8	5.0	5.4	0.4	6.6	1.2	0.5	0.03	0.05	1.78	27	56	0.03	1.4
P14 (2260 m)	A	0–54/59	5YR2.5/2	7.5YR3/3	85	12	3	C	10.4	5.1	4.5	−0.6	56.6	8.4	1.8	0.30	0.08	10.58	19	21	0.50	40.0
	Bw1	54/59–82/90	5YR4/4	7.5YR3/4	95	3	2	C	4.9	5.1	4.7	−0.4	41.4	2.8	0.6	0.20	0.08	3.68	9	11	0.33	30.7
	Bw2	82/90–120/128	5YR4/6	7.5YR3/4	84	13	3	C	4.6	5.0	4.9	−0.1	27.4	1.7	0.5	0.20	0.06	2.46	9	10	0.28	22.9
	2Bo	120/128–140/150	2.5YR3/6	5YR4/6	n.d.	n.d.	n.d.	n.d.	2.9	4.8	4.9	0.1	13.4	1.4	0.7	0.20	0.06	2.36	17	20	0.12	9.7
	2Bcs	140/150–190	10YR3/6	5YR4/6	n.d.	n.d.	n.d.	n.d.	1.8	4.8	5.2	0.4	7.8	1.0	0.9	0.20	0.08	2.18	28	47	0.08	2.5

Table 2
Bulk density (B.D.), phosphorus (P) retention, and extracted elements with acid oxalate (OX), dithionite-citrate-bicarbonate (DCB) and pyrophosphate (PYR).

Pedon (altitude)	Hor.	Depth (cm)	B.D. $Mg \cdot m^{-3}$	P-ret. (%)	OX (%)				DCB (%)		PYR (%)	
					Fe_o	Al_o	$Al_o + 1/2\ Fe_o$	Si_o	Fe_d	Al_d	Fe_p	Al_p
P2 (1500 m)	Ap1	0–6	0.88	59	0.46	0.82	1.05	0.17	9.37	1.86	0.19	0.44
	Ap2	6–18/24	0.89	51	0.44	0.73	0.95	0.13	9.30	1.78	0.22	0.44
	Bt1	18/24–32/34	1.00	56	0.43	0.60	0.82	0.09	9.51	1.71	0.22	0.41
	Bt2	32/34–67	0.92	62	0.40	0.38	0.58	0.04	9.79	1.63	0.03	0.10
	Bt3	67–103	1.07	63	0.46	0.36	0.59	0.04	10.98	1.51	0.01	0.07
	Bt4	103–150	1.05	56	0.45	0.33	0.56	0.04	11.19	1.26	0.01	0.07
P4 (1700 m)	Ap	0–22	0.78	65	0.50	1.30	1.55	0.41	7.13	1.67	0.22	0.74
	AB	22–40/47	1.05	63	0.40	0.67	0.87	0.09	7.55	1.43	0.64	0.70
	Bo1	40/47–70	1.04	55	0.33	0.43	0.60	0.03	8.53	1.22	0.07	0.14
	Bo2	70–108	1.02	58	0.38	0.41	0.60	0.04	9.09	1.08	0.01	0.08
	Bo3	108–136	1.04	59	0.42	0.39	0.60	0.04	9.30	1.05	0.01	0.07
	Bo4	136–190	1.04	60	0.42	0.36	0.57	0.03	9.37	0.95	0.01	0.06
P6 (1780 m)	Ap	0–12/18	0.74	66	0.57	1.23	1.52	0.24	7.52	1.88	0.37	0.83
	BA	12/18–32/39	0.82	49	0.40	0.54	0.74	0.05	8.55	1.37	0.44	0.40
	Bt1	32/39–52/67	0.93	57	0.29	0.37	0.51	0.02	8.68	1.32	0.02	0.09
	Btcs2	52/67–88/100	1.09	58	0.34	0.32	0.49	0.02	9.04	1.05	0.01	0.07
	2Bo1	88/100–110/128	1.03	64	0.35	0.35	0.52	0.03	9.31	0.96	0.01	0.06
	2Bo2	110/128–178	1.04	51	0.29	0.27	0.41	0.03	9.27	0.93	0.01	0.05
P11 (2000 m)	Ap1	0–25/28	0.62	69	0.66	2.02	2.35	0.44	7.41	1.72	0.33	1.16
	Bw1	25/28–44/52	0.64	62	0.71	1.96	2.32	0.57	7.41	1.99	0.31	0.85
	Bw2	44/52–63/72	0.72	64	0.70	1.75	2.10	0.47	7.55	2.14	0.38	0.89
	Bw3	63/72–77/84	0.87	65	0.58	1.21	1.50	0.22	8.18	2.07	0.91	1.43
	2Bo	77/84–190	0.86	58	0.61	0.83	1.13	0.07	9.51	1.84	0.21	0.21
P13 (2120 m)	A1	0–15/25	0.69	84	0.90	2.40	2.85	0.50	6.22	2.53	0.70	1.81
	A2	15/25–42/43	0.65	80	0.97	2.77	3.25	0.64	8.05	2.32	0.73	1.44
	Bw1	42/43–52/54	0.86	70	0.87	1.57	2.00	0.17	8.87	2.23	1.06	1.31
	Bw2	52/54–101	0.86	69	1.15	1.10	1.67	0.07	9.45	1.86	1.20	1.07
	2Bo1	101–131	1.10	56	0.43	0.43	0.65	0.02	9.79	0.98	0.07	0.13
	2Bo2	131–190	1.08	53	0.42	0.26	0.47	0.01	10.66	0.88	0.01	0.06
P14 (2260 m)	Ap	0–54/59	0.61	72	1.29	2.64	3.28	0.69	7.29	2.50	0.71	1.53
	Bw1	54/59–82/90	0.85	58	1.99	2.04	3.04	0.16	10.82	2.93	2.33	2.58
	Bw2	82/90–120/128	1.17	71	1.84	1.51	2.43	0.12	11.71	2.22	1.45	1.42
	2Bo	120/128–140/150	1.09	59	0.91	0.64	1.09	0.05	11.10	1.37	0.90	0.54
	2Bcs	140/150–190	1.12	41	0.48	0.22	0.46	0.02	11.26	0.93	0.71	0.05

Table 3
Results of t-test used to compare the mean values of soil properties between Bw and A horizons and between Bw and Bt-Bo horizons.

Unpaired *t*-test		B.D.	P-ret.	Fe_o	Al_o	$Al_o + 1/2\ Fe_o$	Si_o	Fe_d	Al_d	Fe_p	Al_p	Overall
Is Bw significantly different from A horizons?	t-Statistic	−1.069	0.530	−1.807	0.090	−0.494	1.126	−1.964	−1.308	−2.344	−1.281	−2.768
	p-Value	0.306	0.606	0.106	0.930	0.630	0.279	0.079	0.213	0.051	0.225	0.064
Is Bw significantly different from other B horizons?	t-Statistic	2.747	−4.089	−3.119	−8.458	−7.648	−3.034	0.983	−6.631	−3.571	−5.491	−7.572
	p-Value	0.029	0.001	0.019	6.89E-05	1.41E-04	0.023	0.356	5.56E-05	9.69E-03	1.32E-03	5.13E-11
		*	***	*	***	***	*		***	**	***	***

*** p-value ≤ 0.001; ** 0.001 < p-value ≤ 0.01; * 0.01 < p-value ≤ 0.05.

70° 2θ, at a step of 0.010° 2θ, and a count time of 48 s per step.

The obtained powder diffraction patterns were interpreted qualitatively using the COD database (Downs and Hall-Wallace, 2003; Gražulis et al., 2009, 2012) and quantitatively using the BGMN Rietveld model (Bergmann et al., 1998) with Profex as user interface (Doebelin and Kleeberg, 2015).

3.4. Micromorphological analysis

Undisturbed soil samples were oven-dried (50–60 °C) and subsequently impregnated under vacuum with a cold-setting polyester resin (Benyarku and Stoops, 2005). The thin sections (2.4 × 4.8 cm) were studied with a polarizing microscope and described using the terminology of Stoops (2003).

3.5. Statistical analysis

For statistical analysis, three sets of samples were considered: A horizons, Bw horizons and other B horizons (Bt and Bo). The Student's unpaired t method (Armitage et al., 2001) was used to test the equality of the sample means between Bw and Bt-Bo horizons, and between Bw and A horizons. The equality of means was challenged either per soil characteristic or by combining all soil characteristics (Ye et al., 2008). Measurements of different soil characteristics were standardized before being combined, using Eq. (1):

$$x_i{}' = \frac{x_i - \bar{x}}{\sqrt{\frac{1}{n-1} \cdot \sum_{i=1}^{n} (x_i - \bar{x})^2}} \tag{1}$$

where x is the measured value of a soil characteristic, x′ is the standardized value of x, $\bar{x}$ is the mean of x, $\bar{x} = \frac{1}{n} \sum_{i=1}^{n} x_i$, and n is total number of measurements of the soil characteristic.

The t statistic involving samples 1 and 2 was calculated using Eq. (2):

$$t = \frac{\bar{x}_1{}' - \bar{x}_2{}'}{\sqrt{\frac{1}{n_1 + n_2 - 2} \cdot \left[\sum_{i=1}^{n_1} (x_i{}' - \bar{x}_1{}')^2 + \sum_{j=1}^{n_2} (x_j{}' - \bar{x}_2{}')^2 \right] \cdot \left(\frac{1}{n_1} + \frac{1}{n_2} \right)}} \tag{2}$$

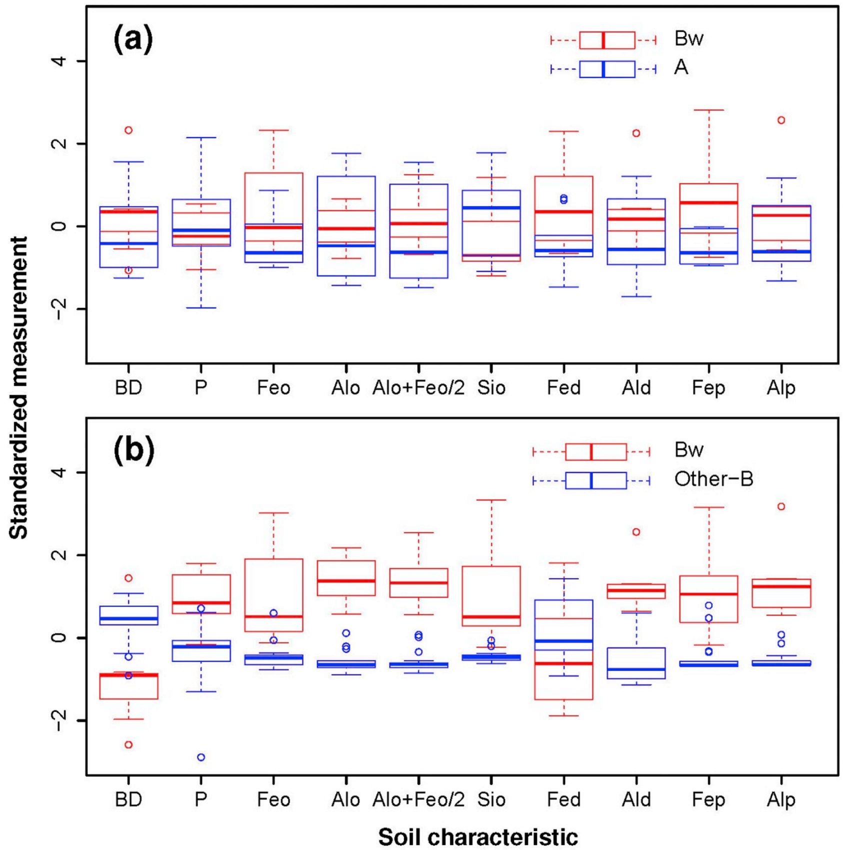

Fig. 3. Vertically aligned boxplot pairs of selected soil characteristics to visualize the comparison between the Bw horizons and (a) the A horizons and (b) the other B horizons. (For interpretation of the references to colour in this figure, the reader is referred to the web version of this article.)

Data processing and analysis were conducted using R v3.3 software (R Core Team, 2016).

4. Results and discussion

4.1. General soil characteristics

Below 1800 m, the selected pedons are characterized by dark red to red Bt or Bo horizons, covered by dark reddish brown to dark brown Ap or A horizons (Table 1). Above 1800 m, the profiles comprise A and Bw horizons with fluffy consistency, becoming thicker with increasing altitude (> 1 m). All soil horizons have a clayey texture, except some topsoils in the lower part of the sequence. The latter have a higher silt content, which can be due to incomplete dispersion, caused by strong microaggregation (Bartoli et al., 1991). The OC content of the soils increases with increasing elevation, reaching values > 10%. The Bw horizons have lower pH-KCl values (< 5) than the Bt and Bo horizons (> 5), which is also reflected by higher extractable acidity values. The CEC positively correlates with OC content. The sum of the base cations is low in the B horizons (< 4 cmol(+) kg^{-1}), except in pedon 11 (2000 m altitude). The values are higher for the A horizons, which can be due to the nutrient biorecycling (Jobbágy and Jackson, 2001) and/or slash-and-burn cultivation (Sanchez, 1976).

4.2. Andic soil properties

Special attention was paid to andic soil properties (BD, P retention, Al_o + 1/2Fe_o) and to other characteristics which could be indicative for volcanic ash as parent material (e.g., Si_o, DCB- and pyrophosphate-extractable Fe and Al) (Table 2). Bulk density is below 0.9 Mg m^{-3} in the A horizons and in nearly all Bw horizons, and it is > 1 in almost all Bt and 2Bo horizons. All horizons have P retention values below the minimum required for andic soil properties (85%), but they are somewhat higher for the Bw horizons than for Bt and Bo horizons. The Al_o + 1/2Fe_o content exceeds the minimum required for andic soil properties (2%) for the A and Bw horizons of pedons P11, P13 and P14, in the high-altitude part of the sequence. These horizons also have higher Al_d, Fe_p and Al_p contents than the 2Bo horizons of the same profiles and than all horizons of the low-altitude pedons (P2, P4, P6). The Bw horizons have slightly higher Si_o contents than the other B horizons, but the values are low (< 0.6%), which is not compatible with the presence of allophanic materials. The Fe_d content is high (7–11%) and gradually decreases with decreasing depth in all pedons.

We used a *t*-test to compare the means of soil property values for pairs of soil horizons (Bw versus Bt-Bo horizons, Bw versus A horizons). The probability (i.e., p-value) associated with the computed statistical value (i.e., t-statistic) is a measure of the likelihood of the means of the two samples being equal. The t-statistic and p-values are reported in Table 3. For example, comparison of the mean bulk density of all Bw horizons to that of the other B horizons yields a t-statistic value of 2.747, with a p-value of 0.029. The average BD of the Bw horizons is significantly different from that of the other B horizons (0.029). In contrast, comparison of BD values between Bw and A horizons yields a t-statistic value of −1.069, with a p-value of 0.306, implying that the Bw and A horizons are similar in terms of bulk density.

To visualize the comparison between the Bw horizons and the other B horizons, and between the Bw and A horizons, Fig. 3 shows vertically aligned boxplot pairs representing all considered soil characteristics (Table 3). The Y-axis shows standardized values for the soil characteristics, allowing visual comparison for parameters that would differ greatly in magnitude without standardization. This exercise shows that the Bw horizons (in red) are different from the other B horizons (in

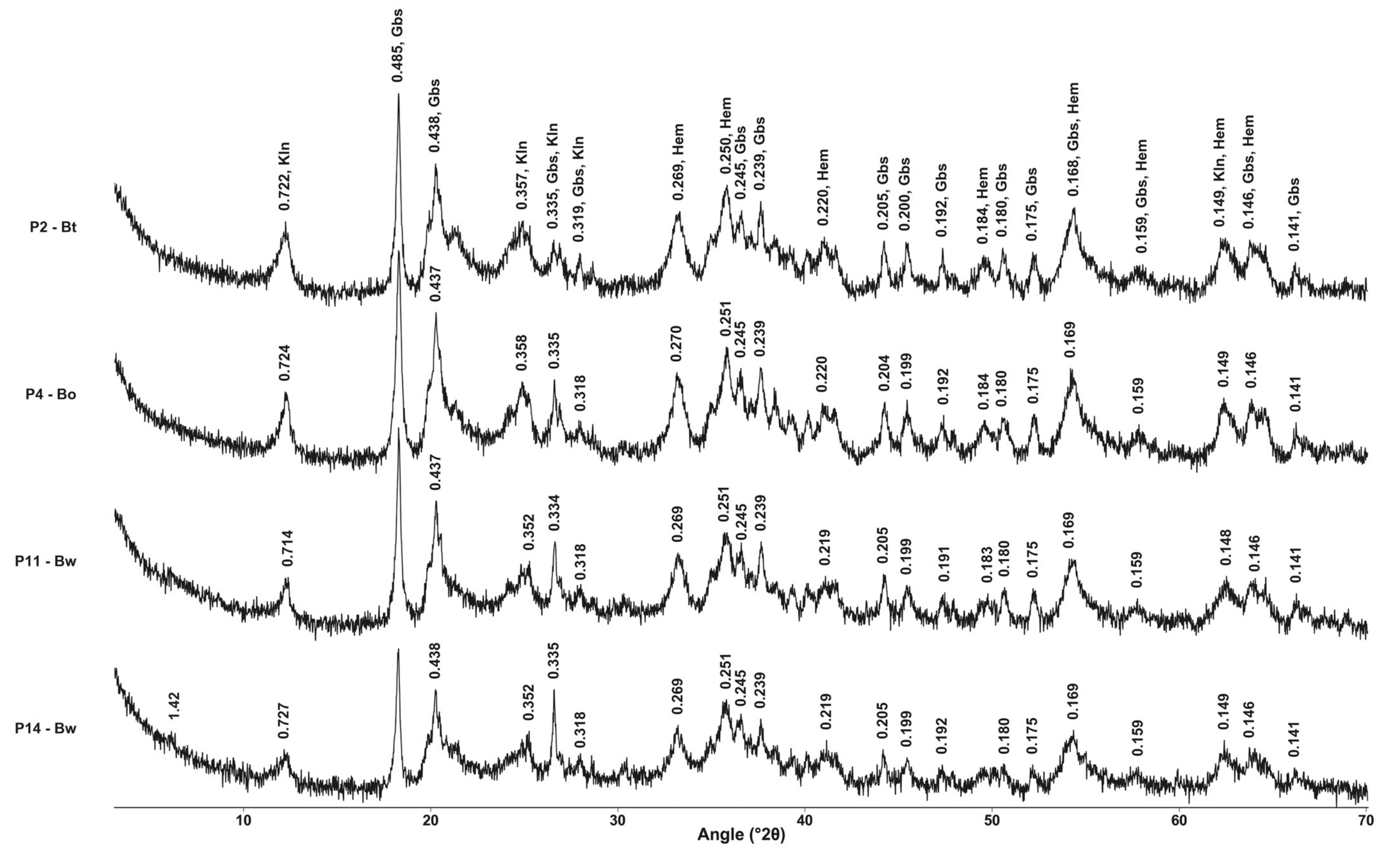

Fig. 4. Powder X-ray diffraction (XRD) patterns for the clay fraction of selected B horizons of studied pedons, d-values are in nm. Abbreviations: Kln: kaolinite, Gbs: gibbsite, Hem: hematite, HIV: hydroxy-interlayered vermiculite.

blue) for all characteristics except Fe_d (Fig. 3). In contrast, the boxplots for Bw horizons (in red) and A horizons (in blue) overlap for all considered soil characteristics (Fig. 3), suggesting that the difference between A and Bw horizons is not statistically significant (see also Table 3).

4.3. Mineralogical properties

Non-quantitative analysis of X-ray powder diffractograms for the clay fraction (Fig. 4) and the silt fraction (Fig. 5) shows that the Bt, Bo and Bw horizons, as well as the A horizons (not shown), have a similar mineralogical composition, with kaolinite and gibbsite as dominant mineral constituents, besides iron oxides (hematite, goethite). Quartz also occurs, as well as traces of feldspar, which is slightly more abundant in the silt fractions. All peaks attributed to gibbsite and goethite disappear after heating the clay samples at 350 °C (Fig. 6). Absence of halloysite-7Å was confirmed by formamide treatment. The small peak at 1.4 nm, disappearing at 350 °C, is attributed to traces of hydroxy-interlayered vermiculite (HIV).

X-ray powder diffractograms for the fine earth fraction (< 2 mm) (Fig. S1) were used to quantify the various mineral constituents (Table 4). The kaolinite content varies between 22 and 41%, the gibbsite content between 18 and 37%, and the [hematite + goethite] content between 17 and 24%. The general trend noticed for the different pedons is a decrease in kaolinite content with increasing depth (unrelated to clay content), whereas gibbsite content shows a progressive increase with increasing depth (Fig. 7). Such a depth-profile of kaolinite and gibbsite contents in ferrallitic soils has been attributed to plant-mediated accumulation of silica in the topsoil (Lucas et al., 1993). More generally, concentration of soil nutrients in the topsoil, relative to subsoil horizons, markedly distinguishes ferrallitic soils from weakly and moderately weathered soils (Jobbágy and Jackson, 2001).

The total elemental analysis data of the fine earth fraction indicate relatively high Al and Fe contents for the A, Bw and Bo horizons of all pedons, associated with Si/(Al + Fe) atomic ratios between 0.91 and 0.34 (Table 5). This clearly denotes strong desilication and reflects the mineralogical composition dominated by kaolinite, gibbsite and iron oxides. The TiO_2 content (2.5 to 4.2%) is compatible with the presence of anatase. The Mg, Ca and K (and Na) contents are very low, indicating only small amounts of ferromagnesian minerals and feldspars. All Bt and Bo horizons, as well as some of the Bw horizons, have TRB values of 40 cmol(+) kg^{-1} or less, which is the upper limit proposed for oxic/ferralic horizons by Herbillon (1986). Other Bw horizons have TRB values between 46 and 85 cmol(+) kg^{-1}, probably due to minor amounts of feldspar and pyroxene, as detected by XRD analysis. The TRB values are greater for A horizons than for the B horizons, which is possibly due the biological cycling of plant nutrients (Jobbágy and Jackson, 2001) and/or slash-and-burn cultivation (Sanchez, 1976).

4.4. Surface charge properties

The soil CEC values corrected for OC and clay contents are indicative of low-activity clays (LAC) exhibiting variable surface charge properties, as previously reported elsewhere (Van Ranst et al., 1998). This explains the low contents of exchangeable base cations (Table 1). The difference between pH_{KCl} and pH_{water} (ΔpH) is −0.8 to +0.4, revealing that the net surface charge can be negative, null or positive depending on the soil horizon. In fact, the relative proportions of organic matter and iron oxides govern charge inversion within a given pedon: OC promotes a negative net surface charge (R^2 = 0.54, Fig. S2) whereas iron oxides (Fe_d) enhance a positive charge (R^2 = 0.48, Fig. S2), as previously reported for basalt-derived Ferralsols in China (Huang et al., 2016). The ΔpH values also indicate that the net surface

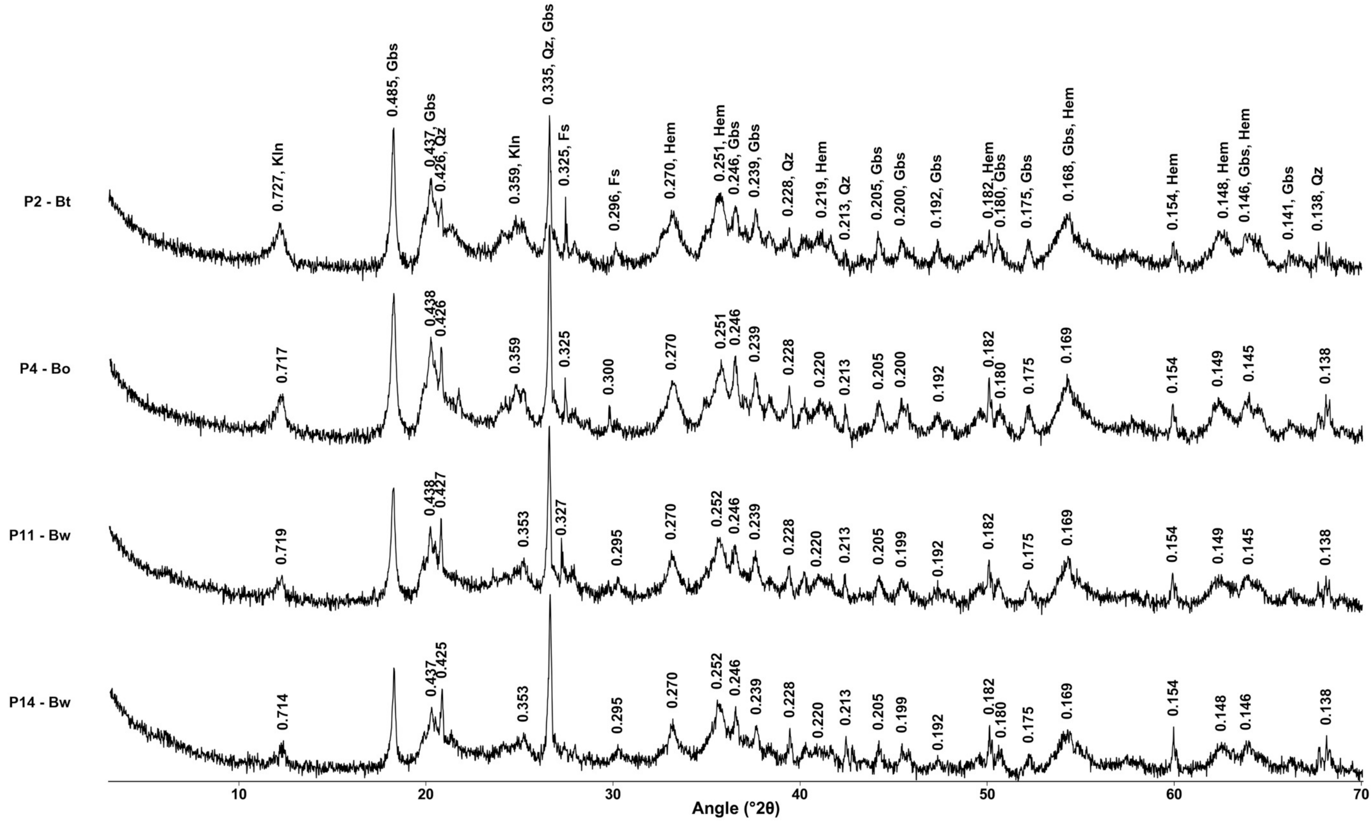

Fig. 5. Powder X-ray diffraction (XRD) patterns for the silt fraction of selected B horizons of studied pedons, d-values are in nm. Abbreviations: Kln kaolinite, Gbs gibbsite, Qz quartz, Fs feldspar, Hem hematite.

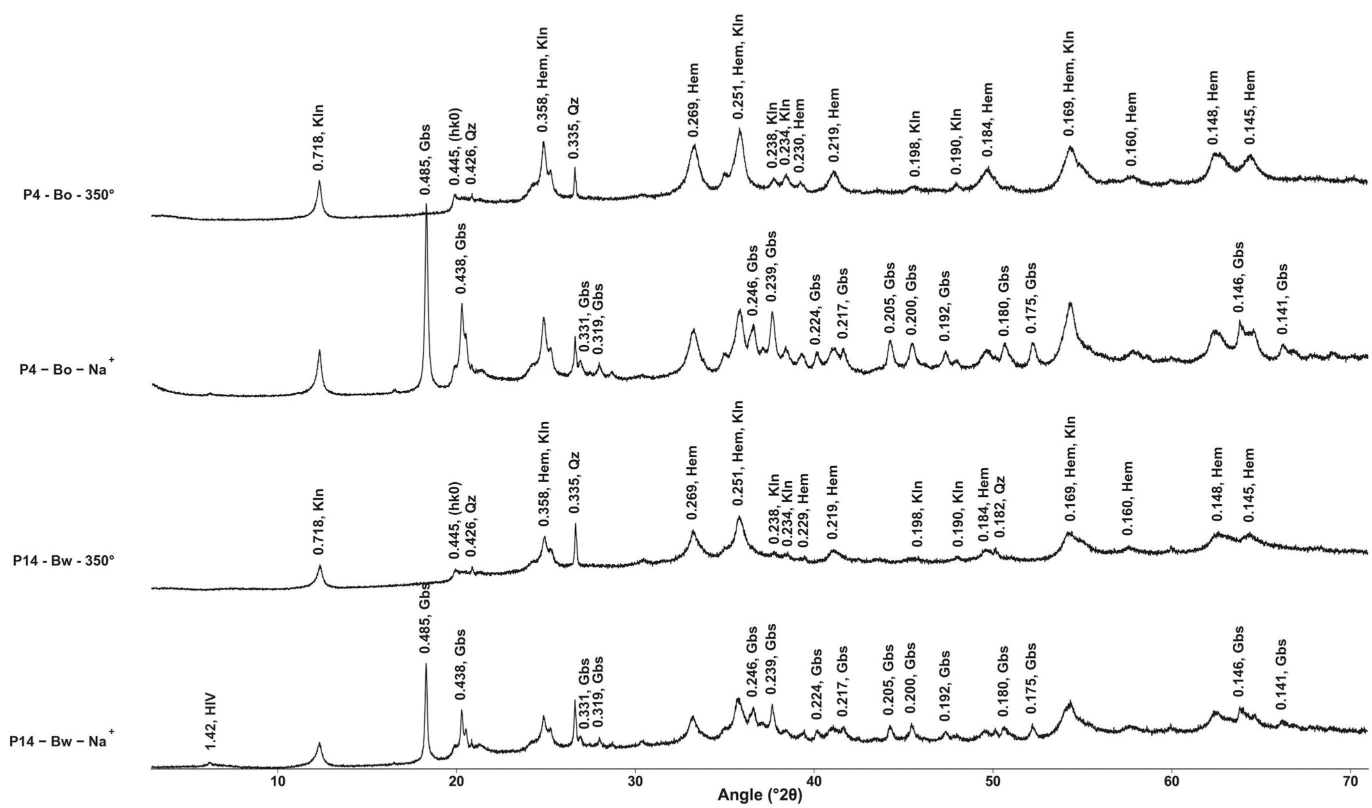

Fig. 6. X-ray diffraction (XRD) patterns for oriented clay samples of Bo horizon of P4 and Bw horizon of P14 before and after heating at 350 °C, d-values are in nm. Abbreviations: Kln: kaolinite, Gbs: gibbsite, Qz: quartz, Hem: hematite, HIV: hydroxy-interlayered vermiculite, hl0: diffraction band related to phyllosilicates.

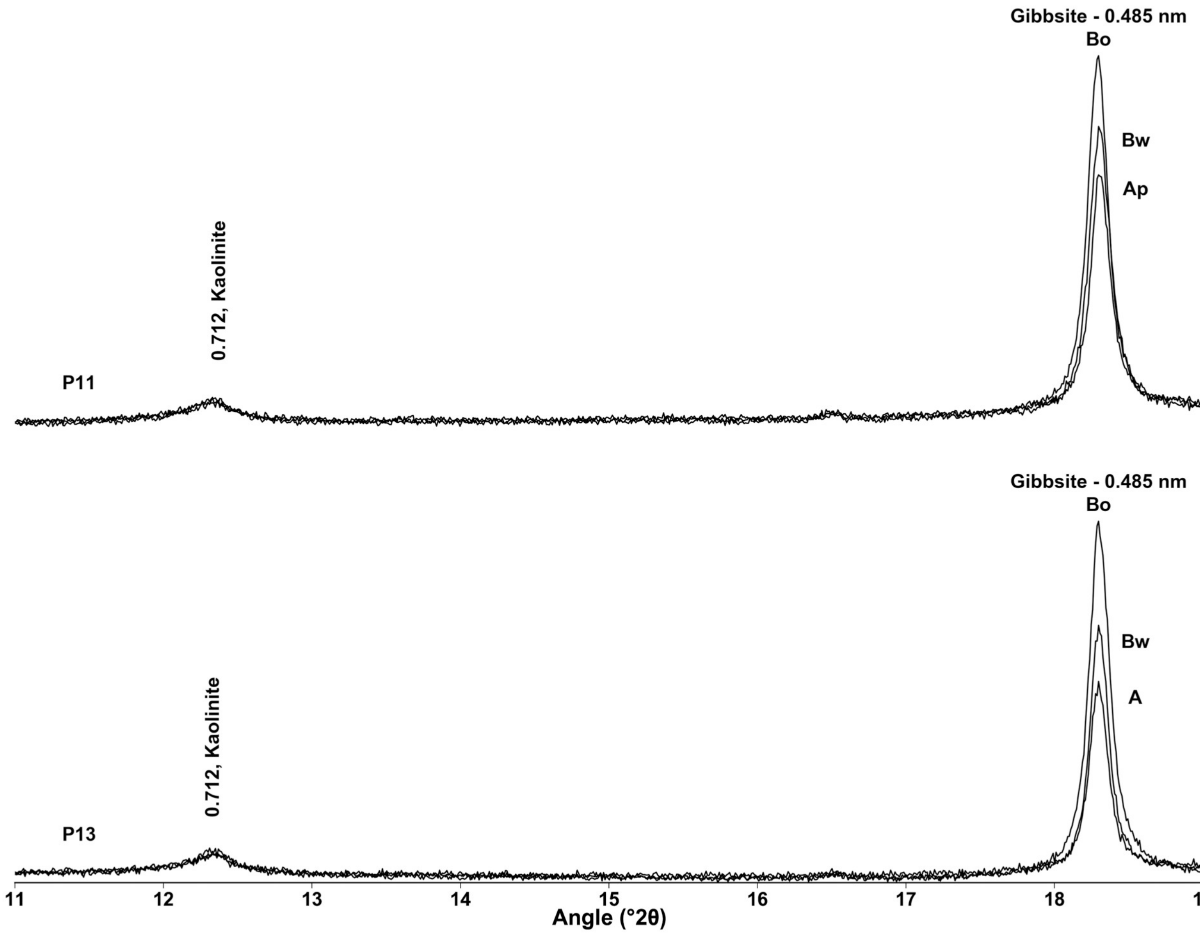

Fig. 7. Powder X-ray diffraction (XRD) patterns for the bulk soil of P11 and P13 showing a decrease in gibbsite content upwards in the pedons.

Table 4
Quantitative mineralogy from Rietveld analysis of powder XRD patterns for bulk soil of selected A and B horizons, in wt%.

Mineral	Pedon 2 (1500 m)			Pedon 4 (1700 m)			Pedon 11 (2000 m)				Pedon 13 (2120 m)		
	Ap2	Bt2	Bt4	AB	Bo1	Bo3	Ap	Bw1	Bw3	2Bo	A2	Bw1	2Bo1
Kaolinite	41	30	35	35	34	27	29	26	25	22	30	26	22
Gibbsite	18	36	30	30	30	37	25	25	31	35	20	26	36
Hematite	16	14	17	17	17	15	13	13	13	12	12	14	13
Goethite	6	3	7	7	5	4	4	4	4	5	5	6	5
Quartz	6	8	5	5	5	9	14	14	15	15	15	16	15
K-Feldspar	5	2	2	2	3	3	5	6	4	5	7	6	4
Plagioclase	2	< 1	< 1	< 1	< 1	< 1	3	3	2	< 1	3	< 1	< 1
Pyroxene	2	< 1	< 1	< 1	< 1	< 1	4	5	< 1	< 1	5	2	< 1
Anatase	< 1	2	2	2	3	3	2	2	2	2	2	2	2
Rutile	< 1	2	< 1	< 1	< 1	2	< 1	< 1	2	2	< 1	2	2
Magnetite	< 1	< 1	< 1	< 1	< 1	< 1	< 1	< 1	< 1	< 1	< 1	< 1	< 1

charge reaches zero in a narrow range of pH_{water} values (4.9–5.5), the lowest pH values being associated with the greatest OC content, as predicted previously (Van Ranst et al., 1998). All soil materials have thus in common an ion exchange complex made of organic matter (OM), kaolinite and Fe/Al oxides characteristic of highly weathered ferrallitic soils. This observation corroborates strong desilication in the Bo and Bt horizons, as supported by very low Si/(Al + Fe) ratios and by low TRB values (Table 5). The proportions of OM and Fe/Al oxides vary with depth, principally with high OM content in topsoils and high concentrations of Fe/Al oxides in subsoil horizons. The OM and iron oxide contents also vary with elevation, with the highest OM content at higher altitudes. As expected, these soils are slightly more acid than those occurring at lower altitudes. Thus, surface charge properties support a common composition of the Bambouto ferrallitic mantle for all pedons of the studied toposequence, the main source of variation being the OM content.

4.5. Micromorphological features

Thin sections were studied for the B horizon of four profiles that are part of the toposequence – pedon 2 (Bt), pedon 4 (Bo), pedon 13 (Bw), and pedon 14 (Bw). The groundmass of all samples is highly similar, with: (i) a very low abundance of coarse material (open porphyric c/f-related distribution pattern, with very low c/f ratio) (Fig. 8a to d), (ii) a silt-dominated coarse fraction, dominated by quartz (with possible presence of feldspar and gibbsite), (iii) a variable minor admixture of

Table 5
Total elemental composition of the fine earth fraction (elements as wt% oxides, loss on ignition as H_2O^- and H_2O^+); total reserve in bases (cmol(+)/kg), TRB; and the atomic ratio Si/(Al + Fe).

Horizon	SiO_2	Al_2O_3	Fe_2O_3	TiO_2	CaO	MgO	K_2O	Na_2O	MnO	P_2O_5	H_2O^-	H_2O^+	Total	TRB	Si/(Al + Fe)
P2-Bt2	19.82	33.10	19.50	3.09	0.10	0.17	0.22	0.08	0.08	0.19	2.50	20.47	99.33	19.47	0.37
P4-Ap	28.45	27.62	12.99	2.30	0.64	0.85	0.35	0.24	0.11	0.24	4.45	22.10	100.34	80.15	0.67
P4-AB	24.94	32.39	14.52	2.54	0.26	0.42	0.27	0.10	0.09	0.14	3.17	20.42	99.29	39.25	0.51
P4-Bo1	22.04	35.77	15.89	2.63	0.09	0.22	0.23	0.04	0.06	0.11	2.38	20.27	99.74	20.24	0.41
P4-Bo3	21.21	36.84	16.60	2.80	0.06	0.19	0.24	0.05	0.05	0.09	2.09	20.44	100.66	18.27	0.38
P6-Bt1	20.11	36.12	17.04	3.31	0.06	0.16	0.11	0.07	0.06	0.14	1.91	20.94	100.03	14.67	0.36
P11-A	26.03	24.88	12.36	2.33	0.62	0.67	0.39	0.18	0.15	0.72	5.97	25.76	100.06	69.42	0.67
P11-Bw1	25.98	26.73	13.09	2.55	0.77	0.87	0.38	0.19	0.14	0.39	6.18	22.35	99.62	84.99	0.63
P11-Bw3	24.58	29.58	14.10	2.70	0.57	0.57	0.37	0.12	0.13	0.30	4.67	21.97	99.65	60.21	0.54
P11-2Bo	23.62	32.24	15.21	2.88	0.32	0.35	0.36	0.13	0.09	0.24	3.82	20.90	100.16	40.54	0.48
P13-A1	23.74	22.56	11.20	2.08	0.49	0.68	0.38	0.18	0.12	0.41	6.99	32.05	100.88	65.07	0.68
P13-Bw1	23.12	30.82	14.89	2.68	0.19	0.41	0.38	0.17	0.11	0.32	5.39	22.19	100.66	40.37	0.49
P13-Bw2	21.95	33.42	15.71	2.79	0.07	0.31	0.33	0.05	0.06	0.20	4.20	20.07	99.16	26.41	0.43
P13-2Bo1	19.40	37.86	15.91	2.81	0.10	0.20	0.42	0.07	0.06	0.17	2.27	20.94	100.21	24.86	0.34
P14-A	28.33	18.13	12.97	2.74	0.69	0.87	0.37	0.20	0.30	0.57	7.51	28.29	100.97	82.06	0.91
P14-Bw1	22.81	25.00	18.01	3.77	0.28	0.43	0.52	0.13	0.16	0.37	6.70	21.98	100.16	46.36	0.53
P14-Bw2	24.36	27.80	18.69	3.77	0.11	0.41	0.36	0.15	0.12	0.26	5.06	18.46	99.56	36.74	0.52
P14-2Bo	21.55	30.91	20.41	4.22	0.13	0.33	0.40	0.08	0.19	0.28	3.04	17.52	99.05	32.38	0.42

sand-sized material, predominantly in the form of quartz and colourless clinopyroxene grains, and (iv) the presence of greyish opal phytoliths (Fig. 8e). The samples from pedons 2, 4 and 13 have an orange brown micromass with weak stipple-speckled b-fabric (see Fig. 8a to c), whereas the micromass of the pedon 14 sample is different in having a dark brown colour (see Fig. 8d). All samples contain few to common rounded aggregates of soil material with a different groundmass than the host material (see Fig. 8c), and some contain altered volcanic rock fragments (pedon 2; Fig. 8f) or reworked bauxitic and lateritic fragments (pedons 2 and 13). The microstructure is largely massive in the Bt and Bo horizon samples, which show channels and vughs as main pore types. In the Bw horizon of pedon 13, the microstructure is massive to coarse-granular (see Fig. 8c), with similar granular aggregates also occurring as distinct channels infillings. The microstructure of the pedon 14 sample has a welded microgranular aspect (see Fig. 8d), whereby similar small granular aggregates again also occur in channels.

Overall, there are no micromorphological indications that the low-altitude profiles (pedons 2 and 4) are derived from a different parent material than the high-altitude profiles (pedons 13 and 14). The groundmass of pedons 13 and 14 shows no features that are compatible with being derived from volcanic ash (cf. Sedov et al., 2010), unless they were entirely erased by strong tropical weathering. The microstructure of the pedon 14 Bw horizon is compatible with its field texture, but its origin is unclear (bioturbation vs aggregation by organic matter).

4.6. Andosolization process and soil classification

The development of surface horizons with high organic matter content (A, Bw) in the high-altitude ferrallitic pedons is related to cool and humid conditions that promote low SOM turnover rates, and to the abundance of potential sources of Al and Fe to form organo-metallic complexes. Humid and cool climates restrict bio-mineralization, thus favouring the accumulation of organic matter in topsoils of highly weathered ferrallitic soils. The sources of Al and Fe are secondary minerals (gibbsite, iron oxides), inherited from a previous cycle of ferrallitisation or lateritic soil formation. The A and Bw horizons of the high-altitude pedons have much higher Al_o, Al_p, Fe_o and Fe_p contents than the underlying 2Bo horizons and than all horizons of the low-altitude pedons. The higher concentration of extractable Al (Al_d, Al_o, Al_p) in the A and Bw horizons can be related to a decreasing amount of gibbsite in these horizons. Gibbsite is known to be particularly unstable in the presence of organic matter (Wilke and Schwertmann, 1977; Madeira and Furtado, 1987; Caner et al., 2000). It is preferentially weathered in soil materials with high organic matter content when mixed with clay minerals such as kaolinite (do Nacimento et al., 2004). Variations in the relative abundance of extractable Fe forms suggests a decrease in crystallinity of the Fe oxides, as well as probable ferrihydrite formation at the expense of more crystalline iron oxides (goethite, hematite), during development of these OM-rich surface horizons. In such horizons, dissolution of iron oxides (mainly hematite and goethite) is commonly enhanced (do Nacimento et al., 2004, 2008; Peretyashko and Sposito, 2006). Weathering of Fe- and Al-bearing minerals by organic acids releases metal cations into soil solutions, in which they are trapped by organic ligands to form organo-metallic complexes. The high metal-to-OC ratios favour immobilization and inhibit downward or downslope transfer of these organo-metallic complexes.

Formation of non-crystalline materials and accumulation of organic matter as dominant pedogenic processes in soils derived from volcanic materials has been named 'andosolization' (Duchaufour, 1977; Ugolini and Dahlgren, 2002).

Increasing andosolization of the originally ferrallitic soils with altitude is well reflected by their soil classification names. In Soil Taxonomy (Soil Survey Staff, 2014), the low-altitude pedons (P2, P4 and P6) have a kandic and/or oxic diagnostic horizon and key out as Kanhapludalf and Kandiudox (Table 6). In WRB (IUSS Working Group WRB, 2015), the same pedons have an argic or ferralic B horizon and key out as Lixisol, Acrisol and Ferralsol (Table 6). In both systems, the pedons are 'Rhodic', reflecting their red colour, and 'Humic', indicating the presence of a humus-rich topsoil.

The high-altitude pedons (P11, P13 and P14), having Bw horizons, do not fulfill the requirements for andic soil properties, because P-retention is below 85%, so they do not qualify as Andisols (Soil Taxonomy) or Andosols (WRB). In Soil Taxonomy, they key out as Dystrudepts and belong to the 'Andic' subgroup because of their low BD ($\leq 1.0\ Mg\ m^{-3}$) and high $Al_o + 1/2Fe_o$ (≥ 1.0). According to WRB, P11 is classified as Cambisol, whereas P13 and P14 are classified as Umbrisols, reflecting the increasing organic matter content with increasing altitude. The set of criteria of the 'Andic' qualifier is not fulfilled for these high-altitude pedons, but the 'Protoandic' subqualifier does apply here. The latter was introduced in WRB in 2014 (IUSS Working Group WRB, 2015), and the limit values for this subqualifier ($BD \leq 1\ Mg\ m^{-3}$, $Al_o + 1/2Fe_o \geq 1.2\%$, P-retention $\geq 55\%$) have been proposed during the 2008 Chile excursion of the IUSS Soil Classification Commission (Peter Schad, pers. comm.).

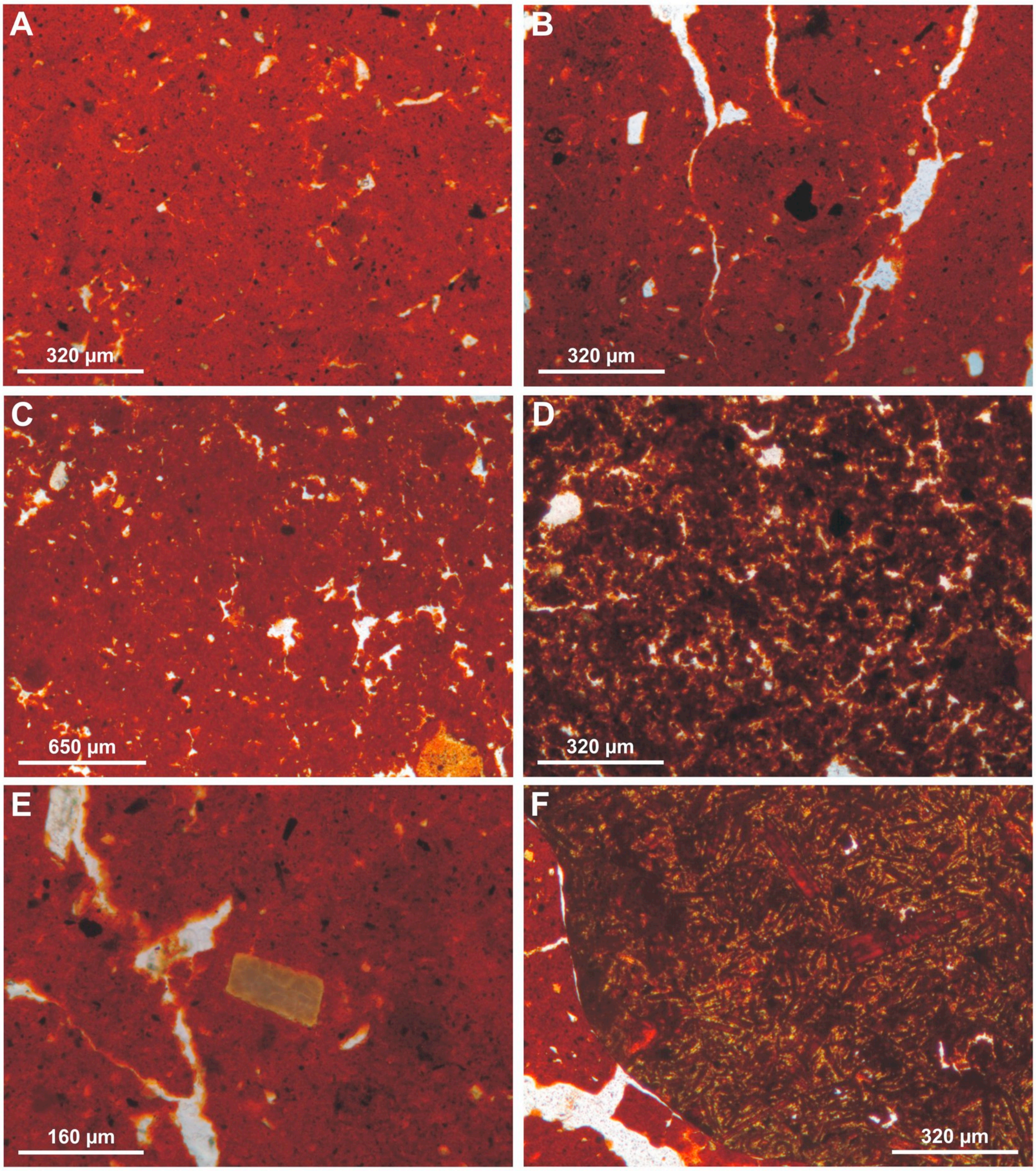

Fig. 8. Micromorphological features. (a) Groundmass of the Bt horizon of P2; (b) Groundmass of the Bo horizon of P4; (c) Groundmass of the Bw horizon of P13, with a microstructure grading to coarse granular and with a rounded aggregate of soil material with a different groundmass composition; (d) Groundmass of the Bw horizon of P14, with fine granular microstructure; (e) Phytolith, in the Bo horizon of P4; (f) Altered volcanic rock fragment, with common pseudomorphs after lath-shaped crystals, in the Bt horizon of P2.

Table 6
Classification of the selected pedons in current international soil classification systems.

Pedon	Soil Taxonomy	World Reference Base
(Altitude)	(Soil Survey Staff, 2014)	(IUSS Working Group WRB, 2015)
P2 (1500 m)	Rhodic Kanhapludalf	Rhodic Lixisol (Clayic, Humic)
P4 (1700 m)	Rhodic Kanhapludalf	Rhodic Acrisol (Clayic, Humic)
P6 (1780 m)	Humic Rhodic Kandiudox	Humic Rhodic Ferralsol (Dystric, Clayic)
P11 (2000 m)	Andic Dystrudept	Dystric Protoandic Cambisol (Clayic, Hyperhumic)
P13 (2120 m)	Andic Dystrudept	Cambic Umbrisol (Protoandic, Clayic, Chromic)
P14 (2260 m)	Andic Dystrudept	Cambic Umbrisol (Protoandic, Clayic, Chromic, Pachic)

5. Conclusions

We developed an integrated approach to understand the development of soil profiles that seem to include a surface horizon of weathered volcanic ash, along the slopes of the Bambouto Mountains, Western Cameroon. Andosolization, or development of (proto)andic properties, characterizes the high-altitude soils (> 1800 m) in the study area. This process results from the strong accumulation of organic material, favoured by environmental conditions in these tropical highlands (grass vegetation, cool humid climate), and by the abundance of residual gibbsite and iron oxides in the highly weathered local soils. Gibbsite and iron oxides are a major source of aluminium and iron that play a crucial role in the stabilization of the organo-metal complexes that are formed. Overall, all analysed properties of the Bw horizons, representing the lower part of the surface interval resembling an altered volcanic ash layer in the field, show a series of features that are not compatible with such an origin. Volcanic ash characteristics could in principle be entirely erased by strong tropical weathering, but this is not in agreement with the observed high degree of similarity between the Bw horizons of the high-altitude pedons and the Bt and Bo horizons of the low-altitude soils, given the assumed relatively young age of any ash that could be present. Earlier studies have documented the development of andic soil properties in strongly weathered tropical soils in non-volcanic settings (Subramanian and Mani, 1981; Caner et al., 2000, 2003, 2007, 2011). Here we present an example of soils at high altitude along the side of a volcano, with surface horizons showing field characteristics and some chemical properties that misleadingly suggest that they are ash-derived andic materials. In studies of soils developed in similar settings, occurring at many localities worldwide, the type of andosolization process should be carefully considered, which will also contribute to correct identification of volcanic parent materials.

Supplementary data to this article can be found online at https://doi.org/10.1016/j.geoderma.2018.12.024.

References

Armitage, P., Berry, G., Matthews, J.N.S., 2001. Statistical Methods in Medical Research, 4th edition. Blackwell Science, Oxford, pp. 817.

Bartoli, F., Burtin, G., Herbillon, A.J., 1991. Disaggregation and clay dispersion of Oxisols: Na-resin, a recommended methodology. Geoderma 49, 301–317.

Benyarku, C.A., Stoops, G., 2005. Guidelines for Preparation of Rock and Soil Thin Sections and Polished Sections. Departament de Medi Ambient i Ciències del Sòl, Universitat de Lleida, Lleida.

Bergmann, J., Friedel, P., Kleeberg, R., 1998. BGMN - a new fundamental parameter based Rietveld program for laboratory X-ray sources, its use in quantitative analysis and structure investigations. In: CPD Newsletter, Commission of Powder Diffraction, International Union of Crystallography. 20. pp. 5–8.

Bitondo, D., Tabi, F.O., Kengmegne, S.S.A., Ngoucheme, M., Mvondo Ze, A.D., 2013. Micronutrient concentrations and environmental concerns in an intensively cultivated Typic Dystrandept in Mount Bambouto, Cameroon. Open J. Soil Sci. 3, 283–288.

Blakemore, L.C., Searle, P.L., Daly, B.K., 1981. Soil bureau laboratory methods: a. methods for chemical analysis of soils. In: New Zealand Soil Bureau Scientific Report, vol. 10A.

Caner, L., Bourgeon, G., Toutain, F., Herbillon, A.J., 2000. Characteristics of non-allophanic Andisols derived from low-activity clay regoliths in the Nilgiri Hills (Southern India). Eur. J. Soil Sci. 51, 553–563.

Caner, L., Toutain, F., Bourgeon, G., Herbillon, A.J., 2003. Occurrence of sombric-like subsurface A horizons in some andic soils of the Nilgiri Hills (Southern India) and their palaeoecological significance. Geoderma 117, 251–265.

Caner, L., Lo Seen, D., Gunnell, Y., Ramesh, B.R., Bourgeon, G., 2007. Spatial heterogeneity of land cover response to climate change in the Nilgiri Hills (southern India) since the last glacial maximum. The Holocene 17, 195–205.

Caner, L., Petit, S., Joussein, E., Fritsch, E., Herbillon, A.J., 2011. Accumulation of organo-metallic complexes in laterites and the formation of Aluandic Andosols in the Nilgiri Hills (southern India): similarities and differences with Umbric Podzols. Eur. J. Soil Sci. 62 (5), 754–764.

Churchman, G.J., Whitton, J.S., Claridge, G.G.C., Theng, B.K.G., 1984. Intercalation method using formamide for differentiating halloysite from kaolinite. Clay Clay Miner. 32 (4), 241–248.

Dahlgren, R.A., 1994. Quantification of allophane and imogolite. In: Amonette, J.E., Zelazny, L.W. (Eds.), Quantitative Methods in Soil Mineralogy. Soil Science Society of America, Madison, pp. 430–451.

Delvaux, B., Herbillon, A.J., Vielvoye, L., 1989. Characterization of a weathering sequence of soils derived from volcanic ash in Cameroon. Taxonomic, mineralogical and agronomic implications. Geoderma 45, 375–388.

do Nacimento, N.R., Bueno, G.T., Fritsch, E., Herbillon, A.J., Allard, T., Melfi, A.J., Astolfo, R., Boucher, H., Li, Y., 2004. Podzolization as a deferralitization process: a study of an Acrisol-Podzol sequence derived from Palaeozoic sandstones in the northern upper Amazon Basin. Eur. J. Soil Sci. 55, 523–538.

do Nacimento, N.R., Fritsch, E., Bueno, G.T., Bardy, M., Grimaldi, C., Melfi, A.J., 2008. Podzolization as a deferralitization process: dynamics and chemistry of ground and surface waters in a Acrisol-Podzol sequence of the upper Amazon Basin. Eur. J. Soil Sci. 59, 911–924.

Doebelin, N., Kleeberg, R., 2015. Profex: a graphical user interface for the Rietveld refinement program BGMN. J. Appl. Crystallogr. 48, 1573–1580.

Doube, M., 1989. Pedogenesis, Classification and Charge Properties of the Bambouto Soil Sequence (West-Cameroon) (Unpublished PhD thesis). State University of Ghent, Faculty of Sciences, Gent, Belgium, pp. 217.

Doube, M., Van Ranst, E., 1984. La pédogenèse comparée et la valeur agricole des sols représentatifs des Hauts-Plateaux de l'Ouest Cameroun. Etude morphologique des profils. MESRES, Centre Univ. Dschang, Dschang, Cameroun, pp. 72.

Downs, R.T., Hall-Wallace, M., 2003. The American Mineralogist crystal structure database. Am. Mineral. 88, 247–250.

Duchaufour, P., 1977. Pédologie. I. Pédogènese et classification. I. Masson, Paris. pp. 496.

Dumort, J.C., 1968. Notice explicative sur la feuille Douala-Ouest. In: Direction des Mines et de la Géologie du Cameroun Yaoundé, pp. 69.

FAO-ISRIC, 1990. Guidelines for profile description, 3rd edition. Food and Agriculture Organization of the United Nations, Rome, Italy.

Gountié Dedzo, M., Nédélec, A., Nono, A., Njanko, T., Font, E., Kamgang, P., Njonfang, E., Launeau, P., 2011. Magnetic fabrics of the Miocene ignimbrites from West-Cameroon: implications for pyroclastic flow source and sedimentation. J. Volcanol. Geotherm. Res. 203, 113–132.

Gražulis, S., Chateigner, D., Downs, R.T., Yokochi, A., Quirós, M., Lutterotti, L., Manakova, E., Butkus, J., Moeck, P., Le Bail, A., 2009. Crystallography Open Database - an open-access collection of crystal structures. J. Appl. Crystallogr. 42, 726–729.

Gražulis, S., Daškevič, A., Merkys, A., Chateigner, D., Lutterotti, L., Quiros, M., Serebryanaya, N.R., Moeck, P., Downs, R.T., Le Bail, A., 2012. Crystallography Open Database (COD): an open-access collection of crystal structures and platform for world-wide collaboration. Nucleic Acids Res. 40, D420–D427.

Herbillon, A.J., 1986. Chemical estimation of weatherable minerals in the diagnostic horizons of low activity clay soils. In: Beinroth, F.H., Camargo, M.N., Eswaran, H. (Eds.), Proceedings of the Eight International Soil Classification Workshop: Classification, Characterization and Utilization of Oxisols, Part 1. EM-BRAPA, Rio de Janeiro, pp. 39–48.

Hieronymus, B., 1972. Etude géologique de quelques types d'altérations dans l'Ouest du Cameroun. 10. Ann. Fac. Sci. du Cameroun, pp. 39–68.

Hillier, S., 1999. Use of an air brush to spray dry samples for X-ray powder diffraction. Clay Miner. 34, 127–135.

Huang, L.M., Zhang, X.H., Shao, M.A., Rossiter, D., Zhang, G.L., 2016. Pedogenesis significantly decreases the stability of water-dispersible soil colloids in a humid tropical region. Geoderma 274, 45–53.

IUSS Working Group WRB, 2015. World Reference Base for Soil Resources 2014, update 2015: International soil classification system for naming soils and creating legends for soil maps. In: World Soil Resources Reports No. 106. FAO, Rome.

Jobbágy, E.G., Jackson, R.B., 2001. The distribution of soil nutrients with depth: global patterns and the imprint of plants. Biogeochemistry 53, 51–77.

Kengni, L., Tekoudjou, H., Tematio, P., Pamo Tedonkeng, E., Tankou, C.M., Lucas, Y., Probst, J.L., 2009. Rainfall variability along the southern flank of the Bambouto mountain (West-Cameroon). J. Cameroon Acad. Sci. 8 (1), 45–52.

Kuété, M., 1999. Exploitation des ressources naturelles dans les environs de Dschang: Impact environmental. In: Vicat, J.P., Bilong, P. (Eds.), Géosciences au Cameroun, Collection Géocam, 2/1999. Presse Univ. de Yaoundé, pp. 47–54.

Lucas, Y., Luizao, F.J., Chauvel, A., Rouiller, J., Nahon, D., 1993. The relation between biological activity of the rain forest and mineral composition of soils. Science 260, 521–523.

Madeira, M., Furtado, A., 1987. The instability of gibbsite and occurrence of other aluminous products in soils of perhumid climate regions of Portugal. In: Garcia de Orta, Serie de Geologia. 10. pp. 35–41.

Marzoli, A., Renne, P.R., Piccirillo, E.M., Francesca, C., Bellieni, G., Melfi, A.J., Nyobe, J.B., N'ni, J., 1999. Silicic magmas from the continental Cameroon Volcanic Line (Oku, Bambouto and Ngaoundéré): $^{40}Ar/^{39}Ar$ dates, petrology, Sr-Nd-O isotopes and their petrogenetic significance. Contrib. Mineral. Petrol. 135 (2–3), 133–150.

Marzoli, A., Piccirillo, E.M., Renne, P.R., Bellieni, G., Iacumin, M., Nyobe, J.B., Tongwa, A.T., 2000. The Cameroon volcanic line revisited: petrogenesis of continental basaltic magmas from lithospheric and asthenospheric mantle source. J. Petrol. 41, 87–109.

Morin, S., 1988. Fundamental dissymmetries of the western Cameroon highlands and their consequences on human occupancy. Case of mount Bambouto. In: Man and Tropical Mountain Review. Sepanrit, Bordeaux, pp. 29–59.

Morin, S., 1989. Hautes terres et bassins de l'Ouest Cameroun. Rev. Géog. Cameroun VIII (2), 81–92 Université de Yaoundé.

N'ni, J., Nyobe, J.B., 1995. Géologie et pétrologie des laves précaldéiriques des monts Bambouto: Ligne du Cameroun. Geochim. Bras. 9, 47–59.

Nono, A., Nkouathio, D.G., Gountié Dedzo, M., Njonfang, E., Kagou Dongmo, A., Tchoua, F.M., 2003. Zonal and vertical variation in welding rate and composition of ignimbrites in the Bambouto volcano (Cameroon Line, Central Africa): volcanological importance. Geophys. Res. Abstr. 5, 14541.

Nono, A., Njonfang, E., Kagou Dongmo, A., Nkouathio, D.G., Tchoua, F.M., 2004. Pyroclastic deposits of the Bambouto volcano (Cameroon Line, Central Africa): evidence of an initial strombolian phase. J. Afr. Earth Sci. 39 (3–5), 409–414.

Peretyashko, T., Sposito, G., 2006. Reducing capacity of terrestrial humic acids. Geoderma 137, 140–158.

R Core Team, 2016. R: A language and environment for statistical computing. R Foundation for Statistical Computing, Vienna, Austria URL. https://www.R-project.org/.

Regnoult, J.M., 1986. Synthèse géologique du Cameroun. Ministère des Mines et de l'Energie. Yaoundé, pp. 119.

Sanchez, P.A., 1976. Properties and Management of Soils in the Tropics. John Wiley and Sons, New York.

Sedov, S., Stoops, G., Shoba, S., 2010. Regoliths and soils on volcanic ash. In: Stoops, G., Marcelino, V., Mees, F. (Eds.), Interpretation of Micromorphological Features of Soils and Regoliths. Elsevier, Amsterdam, pp. 275–303.

Sieffermann, G., 1973. Les sols de quelques régions volcaniques du Cameroun. In: Variations pédologiques du milieu équatorial au milieu tropical. Strasbourg et Mém. ORSTOM, n° 66pp. 183 (Thèse Doct. Sc.).
Siregar, A., Kleber, M., Mikutta, R., Jahn, R., 2005. Sodium hypochlorite oxidation reduces soil organic matter concentrations without affecting inorganic soil constituents. Eur. J. Soil Sci. 56, 481–490.
Soil Survey Staff, 1987. Keys to Soil Taxonomy. 3rd print. Dep. of Agronomy, Cornell University, Agency for International Development, USDA, SMSS, Ithaca, NY.
Soil Survey Staff, 2014. Keys to Soil Taxonomy, 12th edition. USDA and NRCS, pp. 360.
Stoops, G., 2003. Guidelines for Analysis and Description of Soil and Regolith Thin Sections. Soil Science Society of America, Inc. Madison, Wisconsin, USA, pp. 184.
Subramanian, K.S., Mani, G., 1981. Genetic and geomorphic aspects of laterites of high and low landforms in parts of Tamil Nadu, India. In: Proceedings of the International Seminar on Laterisation Processes, Trivandrum. Oxford and IBH Publishing Co., New Delhi & Blakema Rotterdam, pp. 237–245.
Tchoua, F., 1968. Découverte d'ignimbrites dans la région de Dschang (Cameroun). 2. Ann. Fac. Sci. Univ. Féd. Cameroun, Yaoundé, Cameroun, pp. 77–94.
Tchoua, F., 1973. Sur l'existence d'une phase initiale ignimbritique dans le volcanisme des Monts Bambouto (Cameroun). CR Acad. Sci. Paris 276 (D), 2863–2866.
Tchoua, F., 1974. Contribution à l'étude géologique et pétrologique de quelques volcans de la Ligne du Cameroun (Monts Manengouba et Bambouto) (Thèse Doct. Ès Sci.). Univ. Clermont-Ferrand, pp. 346 (unpublished).
Tematio, P., 2005. Etude cartographique et pétrologique des sols à caractères ferrallitiques et andosoliques dans les monts Bambouto (Ouest-Cameroon): influence de la lithologie et des facteurs du milieu sur la nature et la distribution des sols en région de montagne tropicale humide (PhD thesis). Université de Yaoundé I, Cameroun.
Tematio, P., Kengni, L., Bitom, D., Hodson, M., Fopoussi, J.C., Leumbé Leumbé, O., Mpakam, H.G., Tsozué, D., 2004. Soils and their distribution in Bambouto volcanic mountain, West Cameroon Highlands, Central Africa. J. Afr. Earth Sci. 39, 447–457.
Tematio, P., Tsafack, E.I., Kengni, L., 2011. Effects of tillage, fallow and burning on selected properties and fertility status of Andosols in the Mounts Bambouto, West Cameroon. Agric. Sci. 2, 334–340.
Temgoua, E., Djoukoua, J., Likeng, J., Tematio, P., 2014. Structural stability of Andisols and Andic Ferralsols from Mount Bambouto, West Cameroon highlands. Cameroon J. Exp. Biol. 10 (1), 26–34.
Tsozué, D., Bitom, D., Lucas, Y., 2009. Biogeochemistry of iron, aluminium and silicon in humid tropical mountainous soils (Bambouto Mountain, West Cameroon). Open Geol. J. 3, 70–81.
Ugolini, F.C., Dahlgren, R.A., 2002. Soil development in volcanic ash. Glob. Environ. Res. 6, 69–81.
Van Ranst, E., Doube, M., Mvondo Ze, A., Stoops, G., Debaveye, J., 1987. Excursion pédologique dans les Hauts-Plateaux du Cameroun Occidental (Région de Bafou). In: 8ème Réunion de Corrélation des Sols de l'Afrique de l'Ouest et du Centre organisée par la FAO. Centre Univ. Dschang, Discipline des Sciences du Sol, pp. 48.
Van Ranst, E., Shamshuddin, J., Baert, G., Dzwowa, P.K., 1998. Charge characteristics in relation to free iron and organic matter of soils from Bambouto Mountains, Western Cameroon. Eur. J. Soil Sci. 49, 243–252.
van Reeuwijk, L.P., 2002. Procedures for soil analyses. In: Technical Paper 9, 6th edition. ISRIC, Wageningen, The Netherlands, pp. 101.
Wilke, B.M., Schwertmann, U., 1977. Gibbsite and halloysite decomposition in strongly acid podzolic soils developed from granitic saprolite of the bayerischer wald. Geoderma 19, 51–61.
Woolley, A.R., 2001. "Bambouto". Alkaline Rocks and Carbonatites of the World, Part 3. Geological Society, 1-86239-083-5pp. 35.
Ye, L., Tang, H., Zhu, J., Verdoodt, A., Van Ranst, E., 2008. Spatial patterns and effects of soil organic carbon on grain productivity assessment in China. Soil Use Manag. 24, 80–91.
Youmen, D., 1994. Evolution volcanologique, pétrologique et temporelle de la caldéira des monts Bambouto (Cameroun) (Thèse Doctorat). Université Christian Albrecht, Kiel. Faculté Maths et Sciences Naturelles, France, pp. 274.